Small-angle measurement with highly sensitive total-internal-reflection heterodyne interferometer

Jiun-You Lin* and Yu-Cheng Liao

Department of Mechatronics Engineering, National Changhua University of Education, No. 2, Shi-Da Road, Changhua City 50074, Taiwan

*Corresponding author: jylin@cc.ncue.edu.tw

Received 9 September 2013; revised 10 December 2013; accepted 5 February 2014; posted 7 February 2014 (Doc. ID 197368); published 19 March 2014

In this paper, a high-sensitivity total-internal-reflection (TIR) heterodyne interferometer is proposed for measuring small angles. In the proposed interferometer, a half-wave plate and two quarter-wave plates that exhibit specific optic-axis azimuths are combined to form a phase shifter. When a rhomboid prism is placed between the phase shifter and an analyzer that exhibits suitable transmission-axis azimuth, it shifts and enhances the phase difference of the *s*- and *p*-polarization states at double TIR. The enhanced phase difference is dependent on the incident angle; thus small angles can be easily and accurately measured by estimating the phase difference. The experimental results demonstrate the feasibility of this method. Angular resolution and sensitivity levels superior to 1.2×10^{-4} deg (2.1×10^{-6} rad) and 100 (deg/deg), respectively, were attainable in a dynamic range of 0.5 deg. © 2014 Optical Society of America

OCIS codes: (060.2840) Heterodyne; (120.3180) Interferometry; (120.5050) Phase measurement; (260.5430) Polarization; (260.6970) Total internal reflection.

http://dx.doi.org/10.1364/AO.53.001903

1. Introduction

In the precise mechanical industry, optical angle measurement techniques have been extensively applied to the parallelism measurement between two flat surfaces, mechanical system alignment, machine-tool calibration, and mechanical coordinate measurement. For example, if a light is perpendicularly incident to a tested flat reflecting surface and a standard flat reflecting surface, two reflected lights yield an angular difference that can be measured using optical angular measurement; this enables determining the degree of parallelism of a tested surface. Several measurement methods have been proposed, such as laser collimation [1,2], interferometric [3,4], internal-reflection [5,6], and total-internal-reflection (TIR) methods [7–12]. Among these methods, TIR is predominantly adopted. When a light strikes an interface between dense and rare media at an angle larger than the critical angle of the surface normal, the *s* and *p* polarizations of the totally reflected light yield a phase difference based on the angle of incidence. Hence the incident angle and its variation can be detected by measuring the phase difference. Based on the relation between the phase difference and the incident angle, the differential intensity [7,8] and differential TIR heterodyne interferometric methods [9–12] were developed. Regarding the differential intensity method, angular displacement of a light is inferred based on the output intensity change caused by the TIR phase-difference variation. Because the system introduces an initial phase shift and involves a differential optical configuration, the system yields sensitive measurements, excellent linearity, and a low peak-to-peak noise level of nearly

1559-128X/14/091903-06$15.00/0

1.4×10^{-4} deg (2.4×10^{-6} rad), but it is also highly sensitive to the scattering light and the stability of the light source. Regarding the differential TIR heterodyne interferometry, the angle displacement is determined based on the *s*- and *p*-polarization phase difference of the light completely reflected from a TIR prism. Their resolution of approximately 10^{-3} deg ($\sim 1.7 \times 10^{-5}$ rad) can be reached. The method is resistant to environmental disturbances and light source instability, and has high linearity because of its differential common-path configuration and heterodyne phase measurement; however, because the measurement sensitivity of this method depends on the number of TIRs, the design of the TIR prism is critical. In the methods reported by Chiu and Su [9] and Zhou and Cai [10,11], the sensitivity was less than 8 (deg/deg) because of minor TIRs; therefore, the sensitivity of these systems is insufficient for measuring extremely small angles. To enhance the sensitivity, Chiu *et al.* [12] used two elongated parallelogram prisms in a differential configuration, increasing the number of TIRs. In these prisms, the light underwent 20 TIRs, attaining an angular sensitivity greater than 80 (deg/deg); however, compared with the prisms used in the methods proposed by Chiu and Su and Zhou and Cai, this measurement system is bulky. In addition, to accurately measure angles, the elongated prisms must demonstrate excellent parallelism; at similar and low levels of parallelism, the light emerging from the elongated prism has nearly 20 times the angular deviation of the light output from a parallelogram prism that uses only two TIRs. The angular deviation of the light caused by the elongated prisms yields a decrease in the measurement accuracy of the incident angle.

To overcome the drawbacks caused by using elongated parallelogram prisms, a high-sensitivity TIR heterodyne interferometer is proposed for measuring small angles; this method is used to perform absolute measurements of the incident angle. A linearly heterodyne light is guided to propagate through a phase shifter, comprising a half-wave and two quarter-wave plates, subsequently penetrating a rhomboid prism (RP) at an angle larger than the critical angle. The light in the prism undergoes two TIRs, finally passing through an analyzer that extracts the interference signal of the *p*- and *s*-polarized light. When the azimuth angles of the phase shifter wave plates are properly chosen, the final phase difference exhibited by the incident angle of the interference signal is associated with the azimuth angle of the analyzer transmission axis. Regulating the azimuth angle of the analyzer substantially increases the final phase difference; thus, small angles can easily be measured by evaluating the increased phase difference using heterodyne interferometry. A theoretical analysis was conducted to confirm the experimental results of the phase differences and incident angles obtained using the proposed technique, which yielded angular sensitivity and resolution levels greater than 100 (deg/deg) and 1.2×10^{-4} deg (2.1×10^{-6} rad) in the measurement range of 0.5 deg. In addition to using a small TIR prism and yielding a high angular sensitivity, the proposed approach provides various advantages, such as a simple structure, sensitivity tunability, and high-resolution stability, because of its common-path configuration and heterodyne phase measurement.

2. Principle

A. Principle of the Small-Angle Measurement Apparatus

Figure 1 demonstrates the optical configuration of the small-angle measurement apparatus. For convenience, the + z axis is set in the direction of the propagation of light and the x axis is perpendicular to the plane of the paper. A linearly polarized light whose light polarization plane is properly set at an angle θ_p from the x axis exhibits the following Jones vector:

$$E_i = \begin{pmatrix} \cos\theta_p \\ \sin\theta_p \end{pmatrix}. \tag{1}$$

The light is incident on a phase shifter, comprising a half-wave plate H_1 (fast axis at a $\Delta/2$ angle to the x axis) and two quarter-wave plates Q_1 and Q_2 (slow axes at 45 and 0 deg with respect to the x axis), and is subsequently incident at θ_i on one side of a RP mounted on a rotation stage. The base angle and refractive index of the prism are 45 deg and n_p, respectively. The light beam enters the prism at an incidence angle of θ_1 onto the prism/air interface, and is totally reflected twice inside the prism. The relation between the angles θ_i and θ_1 can be determined as follows:

$$\theta_1 = 45° + \sin^{-1}\left(\frac{\sin\theta_i}{n_p}\right). \tag{2}$$

When θ_i exceeds θ_{ic}, which is the angle that makes θ_1 equal to the critical angle θ_{1c}, the light is completely reflected at the prism/air interface. The light output from the prism travels through an analyzer AN_t (the transmission axis is β to the x axis) for interference. The amplitude E_{i1} becomes E_t, as follows:

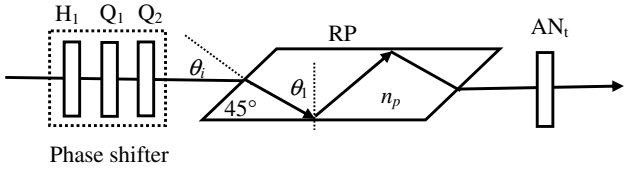

Fig. 1. Total internal reflection in a small-angle measurement apparatus.

$$E_t = \begin{pmatrix} \cos^2\beta & \sin\beta\cos\beta \\ \sin\beta\cos\beta & \sin^2\beta \end{pmatrix} \times \begin{pmatrix} t_a \exp(-i\delta_t/2) & 0 \\ 0 & t_b \exp(i\delta_t/2) \end{pmatrix} \times \begin{pmatrix} 1 & 0 \\ 0 & i \end{pmatrix} \frac{1}{\sqrt{2}} \begin{pmatrix} 1 & -i \\ -i & 1 \end{pmatrix} \times \begin{pmatrix} \cos\Delta & \sin\Delta \\ \sin\Delta & -\cos\Delta \end{pmatrix} \begin{pmatrix} \cos\theta_p \\ \sin\theta_p \end{pmatrix} = (A_{t1}\cos\theta_p \exp(i\phi) + A_{t2}\sin\theta_p \exp(i\pi/2)) \begin{pmatrix} \cos\beta \\ \sin\beta \end{pmatrix}, \tag{3}$$

where the amplitudes A_{t1} and A_{t2} can be written as

$$A_{t1} = \left\{ \frac{1}{2}[(t_p t'_p \cos\beta)^2 + (t_s t'_s \sin\beta)^2 + t_p t'_p t_s t'_s \sin 2\beta \cdot \cos(2\Delta + \delta_t)] \right\}^{1/2}, \tag{4}$$

$$A_{t2} = \left\{ \frac{1}{2}[(t_p t'_p \cos\beta)^2 + (t_s t'_s \sin\beta)^2 - t_p t'_p t_s t'_s \sin 2\beta \cdot \cos(2\Delta + \delta_t)] \right\}^{1/2}, \tag{5}$$

and the phase difference ϕ can be expressed as follows:

$$\phi = \tan^{-1}[-\tan(45° - \sigma) \cdot \tan(\Delta + \delta_t/2)] - \tan^{-1}[-\tan(45° + \sigma) \cdot \tan(\Delta + \delta_t/2)]. \tag{6}$$

In Eqs. (4)–(6), δ_t is the phase difference between the s and p polarizations of two TIRs at the prism/air interface; (t_p, t_s) and (t'_p, t'_s) are the transmission coefficients at the air/prism and prism/air interfaces, respectively; Δ and σ are the parameters introduced using the phase shifter and analyzer ANt, respectively. δ_t and σ can be derived using Fresnel's equations and Jones matrix calculation [13,14]:

$$t_p = \frac{2\cos\theta_i}{n_p\cos\theta_i + [1 - (\sin\theta_i/n_p)^2]^{1/2}}, \tag{9}$$

$$t_s = \frac{2\cos\theta_i}{\cos\theta_i + n_p[1 - (\sin\theta_i/n_p)^2]^{1/2}}, \tag{10}$$

$$t'_p = \frac{2n_p[1 - (\sin\theta_i/n_p)^2]^{1/2}}{n_p\cos\theta_i + [1 - (\sin\theta_i/n_p)^2]^{1/2}}, \tag{11}$$

$$t'_s = \frac{2n_p[1 - (\sin\theta_i/n_p)^2]^{1/2}}{\cos\theta_i + n_p[1 - (\sin\theta_i/n_p)^2]^{1/2}}. \tag{12}$$

As indicated in Eqs. (6)–(12), the phase difference ϕ depends on the parameters of Δ, σ, n_p, and θ_i. If the values of Δ, σ, and n_p are specific, the phase difference ϕ is a function of the incident angle θ_i. Thus, the incident angle θ_i can be estimated by measuring the phase difference ϕ. In the proposed method, Δ is used to vary the phase level of $\delta_t/2$ and is determined based on the azimuth angle of the fast axis of H_1. It must be set at approximately $-\delta_{t,\max}/4$, where $\delta_{t,\max}$ denotes the maximal value of the phase difference δ_t and is expressed as follows [15]:

$$\delta_{t,\max} = 4\tan^{-1}\left(\frac{n_p^2 - 1}{2n_p}\right). \tag{13}$$

The phase-level variation allows the ϕ versus θ_i curve to increase the linearity, extending the measurable range of the incident angle as the parameter σ (determined using β) approaches 45 deg. This increased linearity can enhance the uniformity of the sensitivity when measuring angles. Figure 2 displays the relation between the phase difference ϕ and the incident angle θ_i at an azimuth angle of β when the conditions of $n_p = 1.51509$ and the calculated value $\Delta \cong -\delta_{t,\max}/4 = 23°$ are substituted into Eqs. (6)–(12). For comparison, the relation of the phase difference δ_t versus the incident angle θ_i is also shown in Fig. 2, which indicates that the operating angle β between 0 and 90 deg can regulate the slope of the ϕ versus θ_i curve. At the angles $\beta = 44$ or 46 deg, the phase difference ϕ exhibits sharp and large phase-difference variations around the incident angle θ_{i0} at which the phase difference $(\Delta + \delta_t 2) = 0$ deg. By contrast, the curve δ_t indicates the condition of a small, unchangeable phase-difference variation. According to the simulated results, the system yields high angular

$$\delta_t = 4\tan^{-1}\left\{ \frac{[\sin^2[45° + \sin^{-1}(\sin\theta_i/n_p)] - (1/n_p)^2]^{1/2}}{\tan[45° + \sin^{-1}(\sin\theta_i/n_p)] \cdot \sin[45° + \sin^{-1}(\sin\theta_i/n_p)]} \right\}, \tag{7}$$

$$\sigma = \tan^{-1}\left(\frac{t_s t'_s}{t_p t'_p}\tan\beta\right), \tag{8}$$

and the transmission coefficients are determined as follows:

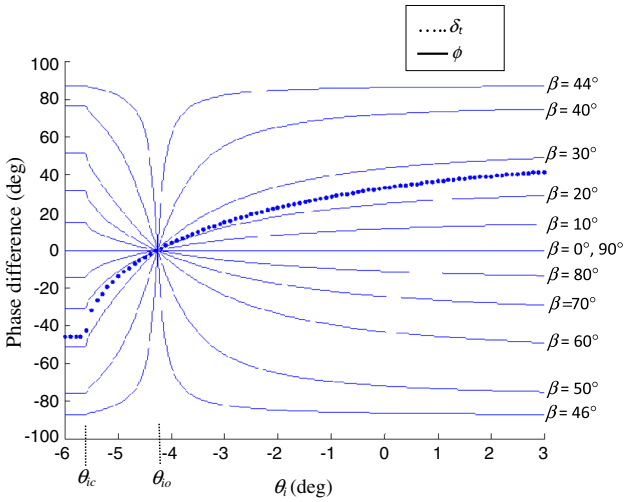

Fig. 2. Phase difference ϕ versus the incident angle θ_i for 0 deg $\le \beta \le$ 90 deg.

sensitivity when the azimuth angle β is near 45 deg. Therefore, small angles can easily be measured when the phase difference ϕ is increased.

B. Phase-Difference Measurement Using Heterodyne Interferometry

Figure 3 shows a schematic diagram of the optical arrangement of the proposed method. A linearly polarized light passes through a half-wave plate H_0, and its polarization plane is at θ_p with respect to the x axis. The light passes through an electro-optic modulator (EO) driven at an angular frequency ω, and is incident on a beam splitter (BS). The BS divides the light into two parts: reflected and transmitted beams. The reflected beam proceeds through an analyzer AN_r at a transmission axis α to the x axis, entering a photodetector D_r. The intensity detected by D_r can be determined based on the following Jones matrix calculation:

$$I_r = \frac{1}{2}[2(\cos\alpha\cos\theta_p)^2 + 2(\sin\alpha\sin\theta_p)^2 + \sin(2\theta_p)\sin(2\alpha)\cos(\omega t - \phi_{BS})], \quad (14)$$

where I_r is the reference signal and ϕ_{BS} is the phase difference between the p and s polarizations

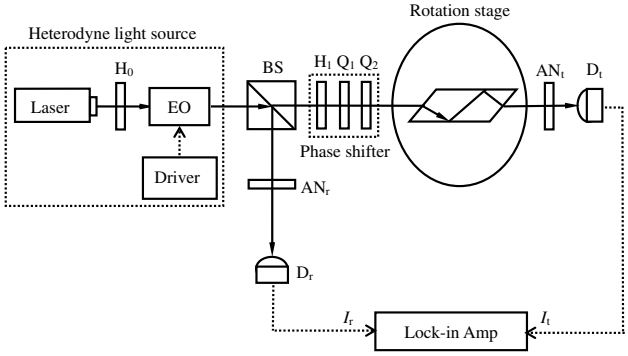

Fig. 3. Schematic diagram of small-angle measurements.

produced by the reflection at the BS. The transmitted beam passes through a phase shifter and penetrates into a RP at θ_i on one side of the prism. After two TIRs, the light output from the prism travels through an analyzer AN_t at a transmission axis β to the x axis, and ends at a photodetector D_t. The intensity of the light detected by D_t can be determined based on Eq. (3),

$$I_t = |E_t|^2 = [(A_{t1}\cos\theta_p)^2 + (A_{t2}\sin\theta_p)^2 + A_{t1}A_{t2}\sin 2\theta_p \cdot \cos(\omega t + \phi - \pi/2)], \quad (15)$$

and I_t is the test signal.

The intensities I_t and I_r are sent to a lock-in amplifier (LIA) for phase analysis, enabling the phase difference

$$\psi = \phi + \phi_{BS} - \pi/2 \quad (16)$$

to be accurately measured. To determine the final difference ϕ, the prism RP and phase shifter are removed, and the test light beam is allowed to travel directly through the analyzer AN_t, entering the detector D_r. After conducting a phase analysis by using a LIA, the phase difference of $\psi = \phi_{BS}$ can be determined. Finally, the value of ϕ_{BS} is substituted into Eq. (16) to determine the phase difference ϕ. Using the measurement data ϕ, and Eqs. (6)–(12) enables estimating the incident angle θ_i.

Although ϕ is independent of θ_p, I_t and I_r depend on θ_p, as indicated in Eqs. (4) and (7). To increase the contrast of I_t and I_r, the following conditions should be applied to the measurement system: (i) α is closed to 0 deg and θ_p is closed to 90 deg as β approaches 44 or 46 deg, and (ii) α and θ_p are closed to 45 deg as β approaches 0 or 90 deg.

3. Experiments and Results

In this experiment, we measured the relation of the phase difference ϕ versus the incident angle θ_i at azimuth angles of $\beta = 20$, 40, and 44 deg. A BK7 RP with $n_p = 1.51509$ was used as a TIR apparatus. The prism was mounted on a high-precision rotational stage (Model SGSP-120YAW, Sigma Koki) at an angular resolution of 0.0025 deg. The wave plate H_1 and analyzer AN_t were fixed in identical precision polarizing rotation holders (Model SPH30, Sigma Koki) at an angular resolution of 0.014 deg. A He–Ne laser with a wavelength of 632.8 nm modulated by an electro-optic modulator (Model 4002, New Focus) was served as the heterodyne light source. The heterodyne light generated a frequency difference of 1 kHz between the p- and s-polarized beams. An LIA (Model SR830, Stanford) that exhibited an angular resolution of 0.01 deg was applied to measure the phase difference. The value of $\Delta \cong -\delta_{t,\max}/4 = -23°$ was determined using Eq. (13), and the azimuth angle of H_1 was set to meet the parameter Δ. To increase the contrast of the signals I_t and I_r, the azimuth angles of $\theta_p = 60$, 80, and 88 deg and $\alpha = 30$, 10, and 2 deg were selected at

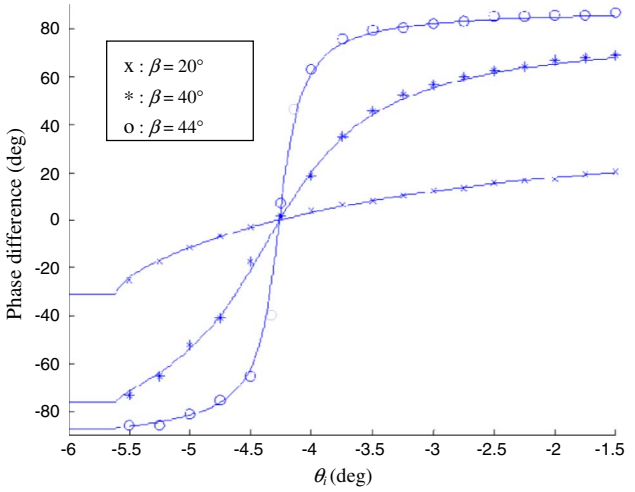

Fig. 4. Measurement results and theoretical curves of ϕ versus θ_i.

$\beta = 20$, 40, and 44 deg, respectively. Figure 4 shows the plotted measurements and theoretical results, where "o," "x," and "∗" represent the measured data, and the solid lines represent the theoretical calculations. The experimental results confirm the theoretically predicted curve, demonstrating that the sensitivity is tunable by changing the orientation of the transmission axis of AN_t. The results also indicate that analyzer azimuth angles of $\beta = 44$ deg yielded high angular sensitivity levels.

4. Discussion

To estimate the angular resolution of the proposed system, we differentiated the equation ϕ; thus, the resolution can be determined as follows:

$$\delta\theta_i = \left|\frac{\partial\theta_i}{\partial\phi}\right|\delta\phi + \left|\frac{\partial\theta_i}{\partial\beta}\right|\delta\Delta + \left|\frac{\partial\theta_i}{\partial\beta}\right|\delta\beta, \tag{17}$$

where $\delta\phi$, $\delta\Delta$, and $\delta\beta$ are the errors in ϕ, Δ, and β, respectively. Considering the angular error of LIA and the periodic nonlinear error [16–19], the net phase-difference error $\Delta\phi$ reduced to $\delta\phi \cong 0.01$ deg. Figure 5 shows the relation of angular resolution $\delta\theta_i$ versus θ_i after substituting the conditions of $\delta\phi \cong 0.01$ deg and $\delta\Delta = \delta\beta = 0.014$ deg (the angular error of the rotation holder) and the experimental results into Eq. (17). The figure indicates that the azimuth $\beta = 44$ deg yields a resolution superior to 1.2×10^{-4} deg $(2.1 \times 10^{-6}$ rad) in the range of -4.5 deg $\le \theta_i \le -4$ deg. In the measurement range of 0.5 deg, the optimal resolution is approximately 2.3×10^{-5} deg $(4 \times 10^{-7}$ rad) at the incident angle $\theta_i = -4.27$ deg. In addition, the sensitivity S of this system is defined as follows:

$$S = \left|\frac{\partial\phi}{\partial\theta_i}\right|. \tag{18}$$

Based on the results shown in Fig. 4, the relations of the sensitivity S versus θ_i are plotted in Fig. 6. At the azimuth angle $\beta = 44$ deg, the angular sensitivity

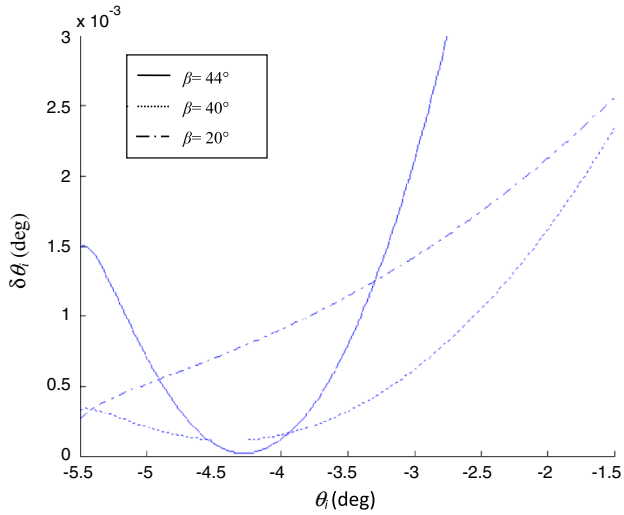

Fig. 5. Angular resolution $\delta\theta_i$ versus the incident angle θ_i.

notably exceeds 100 (deg/deg) in the angle range of -4.5 deg $\le\theta_i \le -4$ deg, and the highest sensitivities are nearly 430 (deg/deg) at the angle $\theta_i = -4.27$ deg. According to the results, the proposed method yields superior resolution and sensitivity compared with those in these methods reported by Zhou *et al.* and Chiu *et al.*

If the phase shifter in the proposed scheme is replaced by a half-wave plate and the fast axis is positioned 22.5 deg to the x axis, the phase difference ϕ can be written as follows by using the Jones matrix calculation:

$$\phi = \tan^{-1}[-\tan(45° - \sigma)\cdot\tan(\delta_t/2)] - \tan^{-1}[-\tan(45° + \sigma)\cdot\tan(\delta_t/2)]. \tag{19}$$

Figure 7 shows the plotted relation between the phase difference ϕ and the incident angle θ_i at azimuth angles of $\beta = 20$, 40, and 44 deg, when a refractive index of $n_p = 1.51509$ is substituted into

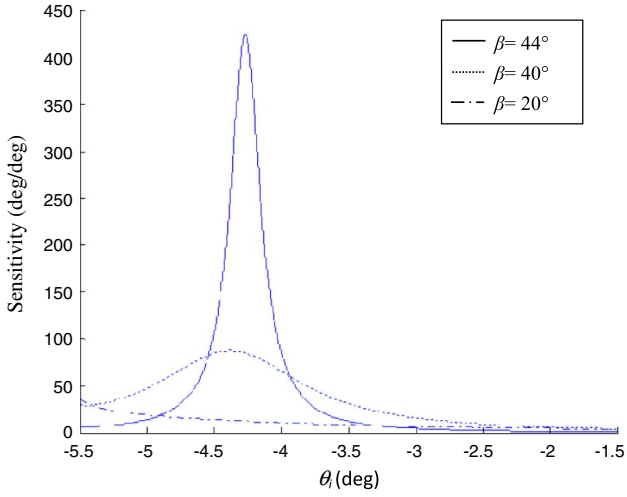

Fig. 6. Sensitivity S versus the incident angle θ_i.

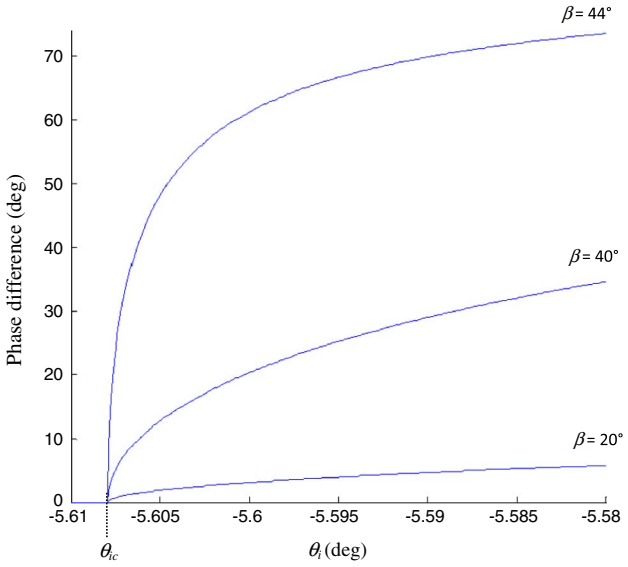

Fig. 7. Phase difference ϕ versus the incident angle θ_i without the phase shifter.

Eq. (19). The figure shows that the phase difference is improved by rotating the transmission axis of the analyzer AN_t; however, its poor linearity and narrow measurable range make it unsuitable for angle measurement.

5. Conclusion

A method for measuring small angles by using highly sensitive TIR interferometry is proposed. The heterodyne interferometer comprises a heterodyne light source, a phase shifter composed of a half-wave and two quarter-wave plates, a RP, and polarization components. Based on the derived phase-difference equations, the relation between the phase difference of the tested signal and the incident angle was examined at various azimuth angles of the transmission axis of the analyzer. The experimental results matched the theoretical analyses. Selecting an azimuth angle of $\beta = 44$ deg for the analyzer of the interferometer can yield an angular resolution and sensitivity superior to 1.2×10^{-4} deg (2.1×10^{-6} rad) and 100 deg/deg, respectively, at a measurable range of 0.5 deg. The proposed approach yields various benefits based on the advantages of common-path and heterodyne interferometry.

The authors thank the National Science Council of the Republic of China, Taiwan, for financially supporting this research under Contract No. 101-2221-E-018-018.

References

1. A. E. Ennos and M. S. Virdee, "High accuracy profile measurement of quasi-conical mirror surface by laser autocollimation," Precis. Eng. **4**, 5–8 (1982).
2. G. G. Luther, R. D. Deslattes, and W. R. Towler, "Single axis photoelectronic autocollimator," Rev. Sci. Instrum. **55**, 747–750 (1984).
3. P. Shi and E. Stijns, "New optical methods for measuring small-angle rotations," Appl. Opt. **27**, 4342–4344 (1988).
4. P. Shi and E. Stijns, "Improving the linearity of the Michelson interferometric angular measurement by a parameter-compensation method," Appl. Opt. **32**, 44–51 (1993).
5. P. S. Huang, S. Kiyono, and O. Kamada, "Angle measurement based on the internal-reflection effect: a new method," Appl. Opt. **31**, 6047–6055 (1992).
6. P. S. Huang and J. Ni, "Angle measurement based on the internal-reflection effect using elongated critical-angle prisms," Appl. Opt. **35**, 2239–2241 (1996).
7. A. Y. Zhang and P. S. Huang, "Total internal reflection for precision small-angle measurement," Appl. Opt. **40**, 1617–1622 (2001).
8. W. Y. Zhang, J. Zhang, and L. Y. Wu, "Small-angle measurement of laser beam steering based on total Internal-reflection effect," J. Phys. Conf. Ser. **48**, 766–770 (2006).
9. M. H. Chiu and D. C. Su, "Improved technique for measuring small angles," Appl. Opt. **36**, 7104–7106 (1997).
10. W. D. Zhou and L. L. Cai, "Interferometer for small-angle measurement based on total internal reflection," Appl. Opt. **37**, 5957–5963 (1998).
11. W. D. Zhou and L. L. Cai, "Improved angle interferometer based on total internal reflection," Appl. Opt. **38**, 1179–1185 (1999).
12. M. H. Chiu, S. F. Wang, and R. S. Chang, "Instrument for measuring small angles by use of multiple total internal reflections in heterodyne interferometry," Appl. Opt. **43**, 5438–5442 (2004).
13. S. F. Wang, M. H. Chiu, W. W. Chen, F. H. Kao, and R. S. Chang, "Small-displacement sensing system based on multiple total internal reflections in heterodyne interferometry," Appl. Opt. **48**, 2566–2573 (2009).
14. E. Hecht, *Optics*, 4th ed. (Addison Wesley, 2002).
15. S. S. Huard, *Polarization of Light* (Wiley, 1997).
16. N. M. Oldham, J. A. Kramar, P. S. Hetrick, and E. C. Teague, "Electronic limitations in phase meters for heterodyne interferometry," Precis. Eng. **15**, 173–179 (1993).
17. J. M. De Freitas and M. A. Player, "Importance of rotational beam alignment in the generation of second harmonic errors in laser heterodyne interferometry," Meas. Sci. Technol. **4**, 1173–1176 (1993).
18. W. Hou and G. Wilkening, "Investigation and compensation of the nonlinearity of heterodyne interferometers," Precis. Eng. **14**, 91–98 (1992).
19. A. E. Rosenbluth and N. Bobroff, "Optical sources of nonlinearity in heterodyne interferometers," Precis. Eng. **12**, 7–11 (1990).